Shahrood University of Technology

Journal of Hydraulic and Water Engineering (JHWE)

Journal homepage: https://jhwe.shahroodut.ac.ir/

Iranian Hydraulic Association (IHA)

Numerical Simulation of Flow Over the Arced Trapezoidal Piano Key Weir

A. Edalati [1,*], R. Amini [2]

[1] Ph.D. Student of Water and Hydraulic Structure, Civil Engineering Collage, Shahrood University of Technology, Shahrood, Iran.
[2] Associate Professor, Department of Water and Environmental Engineering, Civil Engineering Collage, Shahrood University of Technology, Shahrood, Iran.

Article Info

Article history:

Received: 30 April 2023
Received in revised form: 23 Jan 2023
Accepted: 1 Dec 2023
Published online: 3 Dec 2023

DOI:
10.22044/JHWE.2023.13037.1013

Keywords
Piano key weir
Numerical modeling
Multiple regression
Weir angle
Number of cycles

Abstract

A weir is one of the most common man-made hydraulic structures that are used to measure the flow in canals, store water, and control floods. The piano key weir (PKW) is a type of non-linear weir. It is considered one of the best hydraulic-economical options for use in improvement projects to increase the discharge capacity during floods and increase the reservoir volume (by increasing the length of the water passage in a fixed width of the construction) in new dam construction projects. The purpose of this research is to numerically model the flow (using the RNG turbulence model) and investigate the effect of simultaneous changes in the number of cycles and the weir angle on the discharge coefficient by trying to keep the total length of weir crest and other geometric parameters constant for all models. After the investigations, it was found that increasing the weir angle of the PKWs in a fixed length, for all models, increases the discharge coefficient while increasing the number of cycles in a fixed length, leads to the reason for the reduction of the area of the inlet keys, increased contraction of streamlines and the subsequent intensification of the local submergence in the outlet keys, the discharge coefficient will decrease significantly. In the end to predict the changes in the discharge coefficient variable, the conditions of using the multiple regression model, two groups of dimensionless parameters depending on the geometry and flow through the weir were examined and new relationships were presented to calculate the discharge coefficient.

1. Introduction

The intensity of flow in weirs is directly proportional to the length of their crest. Unlike conventional linear weirs, non-linear weirs can increase the flow discharge capacity without increasing the width of the weir without increasing the upstream total head. Meanwhile, a new form of non-linear weirs is Piano Key Weirs (PKWs). PKW has a high discharge capacity and for this reason, it can be used as an economic structure with high efficiency. Recently, various types of weirs have been developed in the same way and used in various dam construction projects. In general, PKW can be divided into 4 types A, B, C, and D, and it should be noted that type A is also the subject of this research. Figure 1 shows the types of PKWs geometric and hydraulic parameters related to the geometry of this type of weir and its structural components.

[*] *Corresponding author:* edalatiadel@yahoo.com, Tel:+989158318983

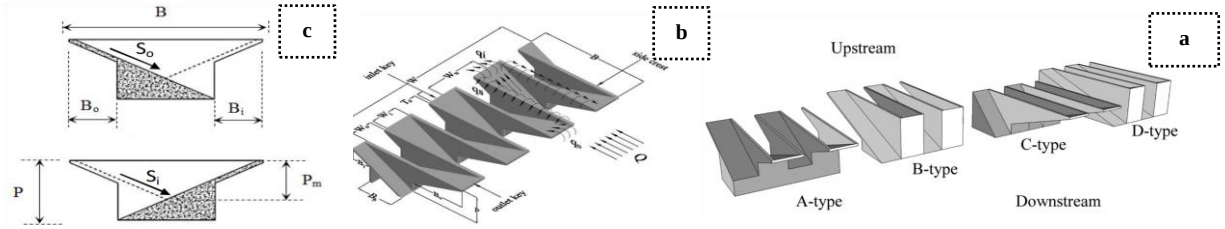

Figure 1. a) types of PKW, **b**) PKW geometric parameters in a three-dimensional view, **c**) PKW geometric parameters in cross-section.

The hydraulic performance of free weirs for a fixed head has a direct relationship with the length of the weir and the discharge coefficient (C_d) of them is calculated using equation (1):

$$C_d = Q/(\frac{2}{3}L\sqrt{2g}H^{1.5}) \quad (1)$$

where L= total length of the weir crest, H = flow head on the weir, and Q = weir discharge. The width limitation in the implementation of conventional and classic free weirs led to their low discharge capacity, therefore labyrinth weirs (non-linear) have been developed as a suitable solution to improve the hydraulic efficiency of these weirs. Labyrinth weirs can increase the flow length (L) within the fixed width of the construction but the vertical shape of the walls of these weirs causes compression of the flows approaching the weir and reduces the hydraulic performance of the weir, for this purpose, a new form of non-linear weirs that are PKWs was provided by the French Hydrocoup Institute and the Hydraulic and Environmental Laboratory of the University of Biscay. Based on Lampreire's laboratory studies, the most optimal value for the width ratio of the inlet key to the outlet key is equal to 1.2. They presented equation (2) as the Head-Discharge relation for piano key weirs. In relation (2), q is the flow rate per unit width, and P_m is height characteristic of the weir (Ouamane and F.Lempérière, 2008).

$$q = 4.3H\sqrt{P_m} \quad (2)$$

Andersen and Tullis (Anderson and Tullis, 2012) investigated the equal height PKWs, labyrinth, and labyrinth with inclined keys with the same rectangular plan. His results showed that in the design of a spillway with restrictions on the width of the channel and the width of the spillway, if a longer length can be created with the limitations of the construction space, even if the curves of the discharge coefficient (C_d) for that geometry are lower than the spillway, the increase in the flow rate in the constant head is quite remarkable. But in general, the curve of discharge coefficient in relation to Ht / P (the ratio of the flow height from the weir to the energy level line to the crest of the weir) of the trapezoidal labyrinth weirs with larger angles is higher than PKWs. Ribeiro et al. (2013) provided an overview of model tests performed on PKW which included research on specific prototypes as well as research models for analyzing system parameters. The main results were (Ribeiro et al., 2013):

- The application of the PKW as an alternative to dam reconstruction and new weir projects has increased over the past years, followed by the creation of an important database of systematic experiments.
- The main parameters to control the discharge capacity of PKWs include L, W, and P_m and H. These parameters have

already been studied in detail by different authors based on systematic tests conducted in laboratory channels.

- The studies of the next years on PKWs operating under free flow conditions will probably focus on analyzing the effect of secondary parameters such as approach conditions, crest shape and thickness, deflection shape under the outlet keys, length of projections, and presence of retaining walls in the outlet keys.

Cicero and Delisle conducted their experiments on simple PKWs with flat crest, half-round, and quarter-round shapes. This analysis confirmed that the effect of the crest shape on the discharge capacity in low heads and semi-round and quarter-round shapes have better hydraulic performance than the performance of the flat shape and concluded that the increase in discharge (related to the flat crest) with increasing height The dam can be effective from 10% to 20% in the downstream head when the scale effects are insignificant (Cicero and Delisle, 2013). Safarzadeh and Norouzi investigated and numerically compared the efficiency, distribution of streamlines, and hydrodynamics of a labyrinth spillway and a rectangular piano key weir (RPKW) with the same plan and reducing local submergence and making the flow distribution more uniform on the crest of a piano weir than a labyrinth weir due to the special geometry. They introduced a piano key weir as the main reason for the high efficiency compared to the labyrinth spillway. In the continuation of this group, by keeping most of the geometric ratios and dimensions of the overflow, including the length of the crest (upstream, downstream, and lateral) they increased the angle of the lateral crest and compared the efficiency and distribution of the rectangular and trapezoidal piano key weir (TPKW[1]) streamlines in the plan. Their results indicated an increase in the discharge coefficient of the TPKW model compared to the RPKW[2] model. The point to consider is the increase in the width of the angular overflow compared to the RPKW model (reduction in L/W) in this case, for a better comparison, the flow rate per unit (q) of the weir width should be considered as a comparison criterion (Safarzadeh and Noroozi, 2017).

Mehboodi et al. conducted extensive laboratory studies on the TPKW and in this study, it was proved that the discharge coefficient of TPKW is 22% higher than the rectangular piano key weir (RPKW). In addition, the effects of TPKW geometric parameters on the discharge coefficient were investigated, which can be summarized as follows (Mehboudi et al., 2016):

- Among the geometrical ratios, Wi/Wo and L/W had the lowest and highest effect in increasing the value of the discharge coefficient (C_d) respectively.
- For a given head (H) the amount of weir discharge increases dramatically for higher values of crest height (P).
- Regardless of the L/W value the maximum value of the discharge coefficient corresponding to the H/P ratio is close to 0.2.
- TPKW can be useful for practical purposes.

Crooksten, Andersen, and Tullis investigated the method of free-flow discharge estimation for PKW geometries. The results of Crooksten et al.'s studies on the validation of the Computational Fluid Dynamics (CFD) method on the PKW showed that the three-dimensional CFD simulation using large eddy simulation (LES[3]) and renormalization group k-ε (RNG[4] k-ε) models for the hydraulic estimation of the PKW with average relative errors of 3 to 4 The percentage is suitable for two test samples and also stated that

[1] Trapezoidal Piano Key Weirs
[2] Rectangular Piano Key Weirs
[3] Large Eddy Simulation
[4] Renormalization Group

experimental data are necessary for the calibration and simulation of CFD results (Crookston et al., 2018). Zinligo et al. compared the formulas for the discharge capacity of PKWs that were developed in the past years and presented a formula based on the available test data. The analysis results showed that the values predicted by the proposed formula are in good agreement with the tested data. with an average error in the range of 5 to 8 percent if the H/P ratio is greater than 0.15. The proposed formula is an easy and practical approach to predicting the release capacity of PKW. Considering the scale effect of a model and the effect of water surface tension, the head ratio in practical applications should be greater than 0.1.

Since there is currently no fixed and practical standard for the design and evaluation of PKW the proposed formula can be used as a reference to evaluate the discharge capacity of type A piano key weir and guide its design. In the case of a small upstream head (usually H/P less than 0.2), the discharge capacity of the PKW is relatively high and the discharge improvement ratio is higher than 3 which indicates an obvious increase in the discharge flow. However, the absolute current is still not high in this case due to the small head. Considering that H/P is less than 1 for normal operations a practical range for the discharge improvement ratio is 1.2 to 3.5. The discharge current decreases. When H/P is greater than 1.2, the flow ratio factor is in the range of 1.2 to 1.3. Therefore, the overflow drain current of the PKW in this sense cannot be increased in a limited way and instead, a reasonable range must be defined for the head. It should be noted that the thickness of the side wall, the height of the shelter on the weir, and the shape of the shelter are secondary factors that may have a small effect on the discharge capacity and their specific effects can be quantified in the next project (Guo et al., 2019). Chartaghi, Nazari, and Shoushtari conducted a laboratory and numerical study of a series with arced-in plan. The comparison of the results obtained for arced trapezoidal piano key weirs (ATPKW[1]) and linear rectangular piano key weirs (LRPKW[2]) showed that, in lower H/P ratios (flow height on the weir to crest height) the LRPKWs showed better performance however increasing the H/P ratio gradually but continuously improves the hydraulic performance of ATPKW models. Reducing the arc angle in the ATPKW models initially reduced the hydraulic performance of these models but later strengthened it significantly (Chahartaghi et al., 2019). Abdul Jabbar Youssef investigated the effect of the side wall angle on the discharge coefficient and the overflow capacity of the PKW in a laboratory manner. He showed that the RPKW works much better than all the non-rectangular models. He stated that increasing the angle of the side wall to 5 and 7 degrees has led to a decrease in the permeability of the overflow to peat by 12 to 18 percent. In addition to this, the results also showed a further decrease in the discharge capacity due to the increase in the angle of the side wall. Finally, he recommended that it is better to conduct more comprehensive research on the effect of the PKW variables with the angle of the side wall in order to optimize its costs and hydraulic performance (Yousif, 2020). Munish Kumar et al. in their laboratory research compared the increased discharge efficiency with TPKW with RPKW and concluded that both have the same L/W ratio. The benefit from synergistic discharge of TPKWs compared to RPKWs was between 2 and 15%. The effect of weir height in increasing the discharge capacity of both types of piano key weirs was positively observed due to the limitation of early immersion of outlet keys with low weirs. In the current research the effect of weir height observed with TPKWs was slightly stronger than RPKWs in influencing hydraulic performance (Kumar et al., 2020).

As it was observed in the history of linear and non-linear weirs, many experimental and

[1] Arced Trapezoidal Piano Key Weirs

[2] Linear Rectangular Piano Key Weirs

laboratory studies have been carried out on PKWs in the field of performance efficiency, dimensions, and optimal sections in reliable laboratories with many facilities and as a result spending a lot of time. It should also be noted that the flow on these weirs is very complex due to the concourse, the slopes, and the special shape of the keys and it is difficult to analyze the effect of various parameters on them because of the number of parameters, these effects It has also become bilateral and it has made it difficult to distinguish the separate effects of each parameter. By looking at this background it seems that there are differences of opinion regarding the form of PKWs in the plan (arced and the linear or non-linear state of these weirs) in such a way that some researchers believe that the PKW is linear and others non-linear, it has been considered superior. Also, by more closely examining the research conducted in recent years on the effect of the changes in the geometrical parameters of the PKW, it can be found that in the laboratory and numerical models presented by the researchers, the geometrical parameters affecting the weir behavior including The total length of the weir, the height of the crest, the width of the inlet and outlet of the weir and the width of the opening of a building are considered in such a way that it could not show the effect of changes in the desired parameter correctly. Nowadays, with the advancement of technology engineers are more looking for the design and simulation of complex spillways with relevant numerical models so that along with very valuable experimental research the information and results of numerical research can also help to solve their problems. In the present research, an attempt has been made to investigate the combined effects of changing the overflow angle and the number of cycles, considering the reduction of the multifaceted effects of other geometric parameters with the help of numerical modeling. For this purpose, in the first step, numerical modeling was done by using the laboratory results of one of Anderson's models (Anderson and Tullis, 2012), and validation of the numerical model was performed by examining two turbulence models RNG and LES. Then in the second step after validation of the numerical model and selection of the best turbulence model, the influence of changes in the geometrical parameters of the weir angle and the number of cycles was also investigated and in the last step, by analyzing the obtained results, the effect of the combined changes of the weir angle and the number of cycles on the weirs coefficient was determined and then the optimal weir with better efficiency was introduced.

2. Equations used in the numerical model

Fluid flow equations are actually the laws of mass conservation and magnitude of motion, which are written as partial differential equations. In order to obtain the flow equations, three steps must be taken. The first step is choosing the correct basic rules, the second step is applying the rules by a suitable flow model, and the third step is learning the mathematical equations that represent the mentioned physical laws. The main equations are four differential equations including continuity relations and magnitude of motion in directions.

2.1. Continuity equation

The mass continuity equation can be written as follows:

$$V_f \frac{\partial \rho}{\partial t} + \frac{\partial}{\partial x}(\rho u A_x) + \frac{\partial}{\partial y}(\rho v A_y) + \frac{\partial}{\partial z}(\rho w A_z) = 0 \qquad (3)$$

which V_f fluid volume fraction, ρ = fluid density, and velocity components (u, v, w) in (x, y, z) directions. The A_x = open area fraction is in x direction, and similarly A_y and A_z = area fraction in (y, z) directions.

2.2. Momentum equation

The equations of motion for the fluid velocity components (u, v, w) in three coordinate directions, or in other words the Navier-Stokes equations, are the relationships shown in equations (4):

$$\begin{aligned}
&\frac{\partial u}{\partial t}+\frac{1}{V_f}\left(uA_x\frac{\partial u}{\partial x}+vA_y\frac{\partial u}{\partial y}+wA_z\frac{\partial u}{\partial z}\right)\\
&\qquad=-\frac{1}{\rho}\frac{\partial P}{\partial x}+G_x+f_x\\
&\frac{\partial v}{\partial t}+\frac{1}{V_f}\left(uA_x\frac{\partial v}{\partial x}+vA_y\frac{\partial v}{\partial y}+wA_z\frac{\partial v}{\partial z}\right)\\
&\qquad=-\frac{1}{\rho}\frac{\partial P}{\partial y}+G_y+f_y\\
&\frac{\partial w}{\partial t}+\frac{1}{V_f}\left(uA_x\frac{\partial w}{\partial x}+vA_y\frac{\partial w}{\partial y}+wA_z\frac{\partial w}{\partial z}\right)\\
&\qquad=-\frac{1}{\rho}\frac{\partial P}{\partial z}+G_z+f_z
\end{aligned} \tag{4}$$

In these equations (G_x, G_y, G_z) are mass accelerations and (f_x, f_y, f_z) are viscous accelerations for dynamic viscosity variables (μ), viscous accelerations are in the form of equations (5):

$$\begin{aligned}
\rho V_f f_x &= wsx-\left\{\frac{\partial}{\partial x}(A_x\tau_{xx})+\frac{\partial}{\partial y}(A_y\tau_{xy})\right.\\
&\quad\left.+\frac{\partial}{\partial z}(A_z\tau_{xz})\right\}\\
\rho V_f f_y &= wsy-\left\{\frac{\partial}{\partial x}(A_x\tau_{xy})+\frac{\partial}{\partial y}(A_y\tau_{yy})\right.\\
&\quad\left.+\frac{\partial}{\partial z}(A_z\tau_{yz})\right\}\\
\rho V_f f_z &= wsz-\left\{\frac{\partial}{\partial x}(A_x\tau_{xz})+\frac{\partial}{\partial y}(A_y\tau_{yz})\right.\\
&\quad\left.+\frac{\partial}{\partial z}(A_z\tau_{zz})\right\}
\end{aligned} \tag{5}$$

In equations (5), the terms *wsx*, *wsy* and *wsz* represent the shear stresses of the walls. If these terms are omitted, there is no wall shear stress because the remaining terms include the fractions of the flow areas (A_x, A_y, A_z), where the walls are not considered. The stresses on the walls are simulated by assuming zero tangential velocity in a part of the surface limited to the flow. Grid and boundaries of moving obstacles are exceptions because they have non-zero tangential velocity.

3. Materials and methods

3.1. Validation of the numerical model for simulating the flow on the PKW

In this part, the analysis of the results of setting the numerical model and its comparison with the results of the corresponding laboratory model conducted by Anderson have been discussed. In the present study, a laboratory model, which will be mentioned later, is considered as the adjusted basic model. For this purpose, numerical model validation using laboratory data is provided.

3.1.1. Laboratory data of PKW

Table 1 contains the geometrical details of the PKW of the essential settings. Also, in this table, the values are in meters, and Figure 2 shows the geometrical parameters mentioned in Table 1 in the form of a figure. Numerical modeling has been done for 5 flow rates from 0.064 to 0.20 cubic meters per second. It should be noted that to simulate the discharge, the initial upstream condition is applied, then the flow head on the weir is extracted as the output. For ease and better understanding, the scenarios are assigned codes. In these codes, the first letter is the initial condition and the second letter represents the parameter output from the model. Also, the subtitle is the main name of the number of the analyzes performed.

Table 1. Geometric characteristics of the RPKW used to validate the numerical model (dimensions in meters).

Parameter	Symbol	Rating
Weir height	**P**	0.196
The length of the overflow crest	**L**	4.745
Channel width	**W**	0.932
Input key width	**Wi**	0.129
Output key width	**Wo**	0.129
The slope of the entrance key floor	**Si**	55.56%
The slope of the bottom of the exit key	**So**	55.56%
Weir width	**lc**	0.489
The length of the entrance console	**Bi**	0.121
The length of the outlet console	**Bo**	0.121
The thickness of the overflow wall	**T**	0.012
Number of cycles	**N**	4
The ratio of the length of the overflow crest to the width of the channel	**L/W**	5.090
The ratio of the width of the inlet key to the outlet key	**Wi/Wo**	1
The ratio of the width of the overflow to the length of the crest	**lc/L**	0.100

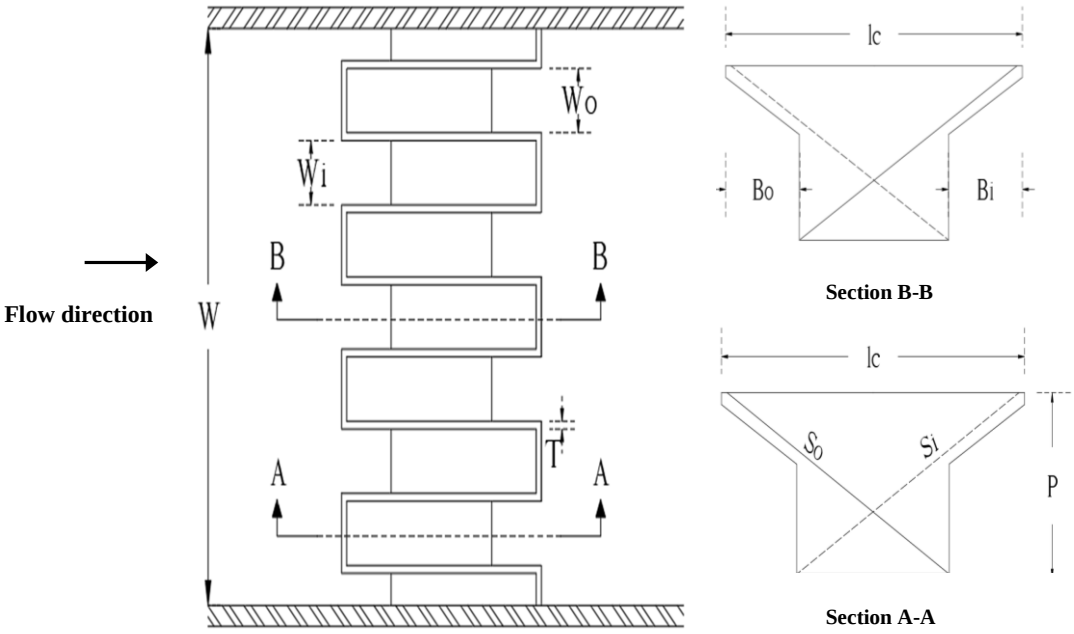

Figure 2. Geometrical parameters of RPKW.

Table 2. Geometric characteristics of RPKW used to validate the numerical model (dimensions in meters).

Simulation code	Flow rate (m^3/s)
Q - H_1	0.064
Q - H_2	0.100
Q - H_3	0.142
Q - H_4	0.166
Q - H_5	0.200

3.2. Boundary conditions

In order to achieve acceptable results, appropriate boundary conditions should be selected, corresponding to the actual laboratory conditions. In order to develop the inlet velocity profile as much as possible, the inlet boundary condition must have a sufficient distance from the weir structure, for this purpose, trial and error has been made in this field. The numerical model has three non-uniform grid blocks with the number of grids along (x, y, z). Figure 3 shows how to grid the 3D solution field. The optimal grid for each block is determined according to the sensitivity of that block's location and also with the help of the GCI[1] algorithm (Roache, 1994). In the mentioned algorithm, this parameter was selected as the target according to the laboratory discharge value, then the optimal network was selected for each block using different grids. Obviously, the block related to the weir structure has more sensitivity and it is necessary to observe and check all the changes in the flow on the weir as much as possible. After using the GCI algorithm, the optimal grid number (30*76*106) was selected for the upstream block, (58*148*94) for the middle block and (35*88*104) for the downstream block. In the following and in Table 3 the boundary conditions used in the blocks can be seen. Figure 4 shows the boundary conditions used in the numerical model.

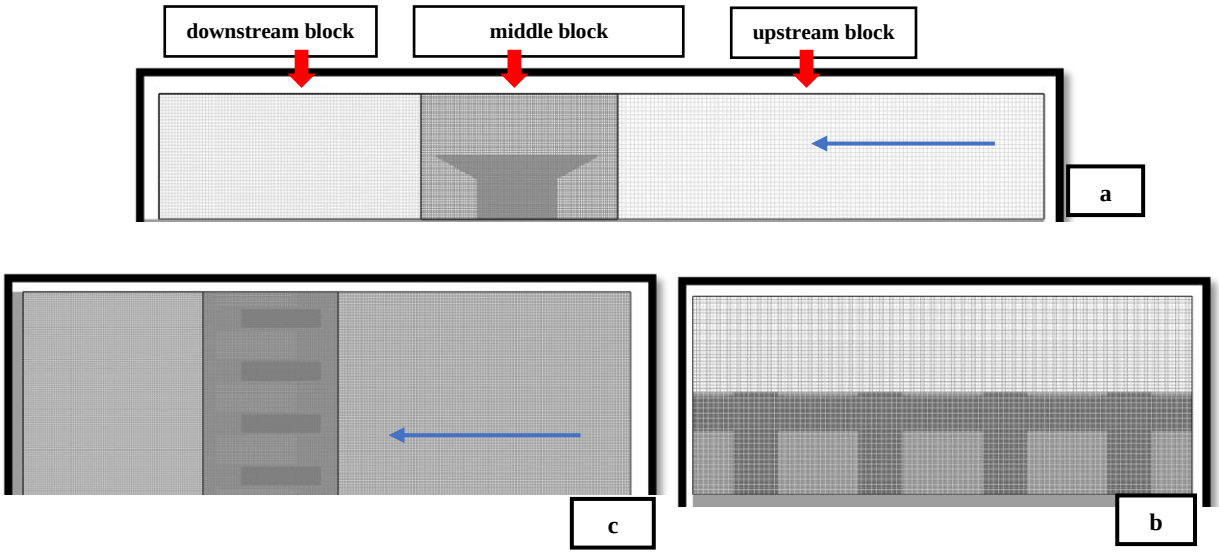

Figure 3. Gridding of the three-dimensional solution field of PKW **a**) xz plane **b**) yz plane **c**) xy plane.

[1] Grid Convergence Index

Table 3. Boundary conditions used in grid blocks.

Block name	Reason for selection	Boundary condition	Vector
Upstream	Entry of flow rate as a prerequisite to the canal	**Volume Flow Rate**	$\mathbf{X_{min}}$
	Connect to the next block	**Symetry**	$\mathbf{X_{max}}$
	Symmetry in Δy/2	**Symetry**	$\mathbf{Y_{min}}$
	Symmetry in Δy/2	**Symetry**	$\mathbf{Y_{max}}$
	Rigid floor overflow	**Wall**	$\mathbf{Z_{min}}$
	Communication with the atmosphere	**Symetry**	$\mathbf{Z_{max}}$
Intermediate (Structural)	The outputs of the solution field are transferred to the next block without any changes	**Continuative**	$\mathbf{X_{min}}$
	Connect to the next block	**Symetry**	$\mathbf{X_{max}}$
	Symmetry in Δy/2	**Symetry**	$\mathbf{Y_{min}}$
	Symmetry in Δy/2	**Symetry**	$\mathbf{Y_{max}}$
	Rigid floor overflow	**Symetry**	$\mathbf{Z_{min}}$
	Communication with the atmosphere	**Symetry**	$\mathbf{Z_{max}}$
Downstream	The outputs of the solution field are transferred to the next block without any changes	**Continuative**	$\mathbf{X_{min}}$
	Outgoing information has reached the border without any change	**Outflow**	$\mathbf{X_{max}}$
	Symmetry in Δy/2	**Symetry**	$\mathbf{Y_{min}}$
	Symmetry in Δy/2	**Symetry**	$\mathbf{Y_{max}}$
	Rigid floor overflow	**Wall**	$\mathbf{Z_{min}}$
	Communication with the atmosphere	**Symetry**	$\mathbf{Z_{max}}$

3.2.1. Choice of turbulence model

One of the most important steps in the numerical modeling of the flow is the selection of the appropriate turbulence model, and in most natural phenomena, the fluid flow is turbulent. Turbulent flow is a type of fluid flow, in which the fluid undergoes strong mixing processes. In this research, RNG and LES turbulence models have been used to model the flow for the same grid for both models. In order to validate the numerical model, the upstream flow head diagram of the weir laboratory sample has been determined for different flow rates and compared with the laboratory results in Figure 4. Figure 4 includes the calculated head using equation (1). According to Figure 4, the results of the numerical method, especially the RNG turbulence model, are in good agreement with the laboratory results and equation (2), although it should be noted that in general, the LES method can provide more accurate results than the RNG method but it requires a high computational cost and a finer grid. As stated in the previous sections, a fixed grid has been considered for both methods. In order to quantitatively compare the results of the numerical model with the laboratory model, parameters should be selected and used as criteria. These criteria in the current study include mean absolute error (MAE), coefficient of determination (R^2), and root mean square error (RMSE). In the mentioned criteria, O represents the observed value of the parameter according to the data of the

laboratory model and P represents the predicted value. It is seen that the parameter is according to the output of the numerical model and N is the number of the examined scenarios. The related relationships are presented in Table 3. According to Table 4, the small values of the mean absolute error and the root mean squared error of the data obtained from the numerical model have little difference from the experimental values, also the high value of the coefficient of determination indicates a very good agreement between the changes in the flow head, total head, and discharge coefficient between the models. numerical and laboratory results.

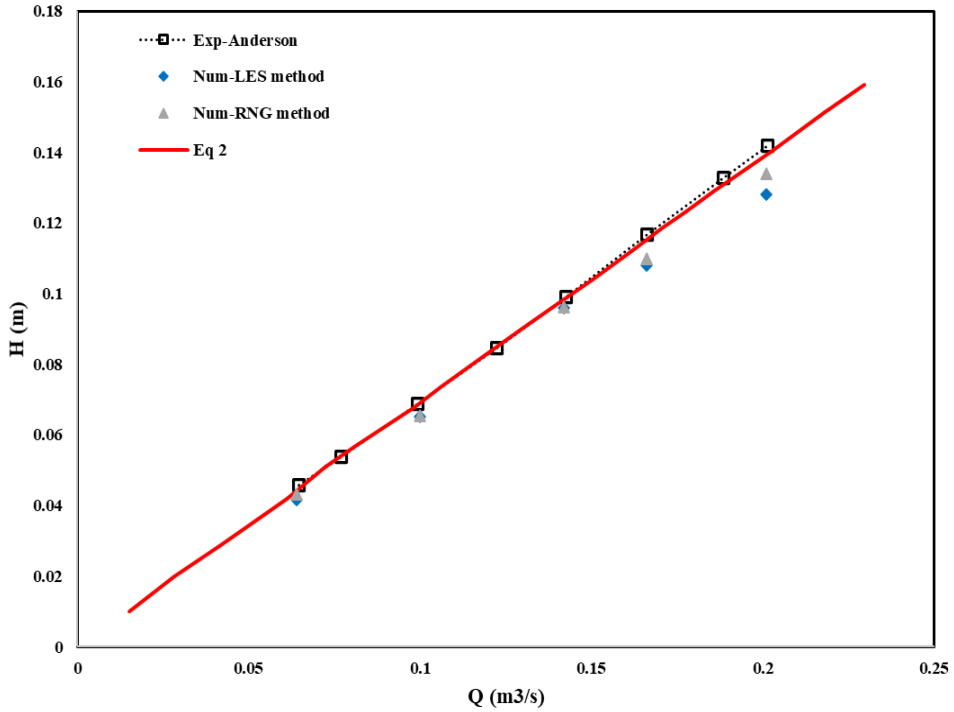

Figure 4. Comparison of changes in water head relative to discharge in the weir according to the specifications of Table 1 between the laboratory data and the numerical model for the Q-H_3 scenario.

Table 4. The criteria used in evaluating the results of the numerical model of the laboratory sample.

parameter	Relationship
MAE	$\frac{\sum\|O-P\|}{N}$
RMSE	$\sqrt{\frac{\sum(O-P)^2}{N}}$
R^2	$1-\frac{\|O-P\|^2}{O^2-\frac{\sum P^2}{N}}$

Table 5. The values of different statistics in order to compare the results of the numerical model with the laboratory data.

R2	MAE	RSME	(RNG) Numerical model			
	H		Q	H	H_t	C_d
0.973	0.0046	0.0051	0.0640	0.0430	0.0478	0.3527
	H_t		0.1000	0.0654	0.0745	0.2833
0.9812	0.0016	0.0019	0.1420	0.0962	0.1098	0.2249
	C_d		0.1660	0.1100	0.1286	0.2057
0.9838	0.0075	0.0080	0.2010	0.1340	0.1580	0.1880
R2	**MAE**	**RSME**	**(LES) Numerical model**			
	H		Q	H	H_t	C_d
0.9569	0.0067	0.0078	0.0640	0.0416	0.0455	0.3799
	H_t		0.1000	0.0651	0.0732	0.2912
0.9760	0.0015	0.0020	0.1420	0.0959	0.1087	0.2284
	C_d		0.1660	0.1080	0.1264	0.2129
0.9749	0.0065	0.0091	0.2010	0.1280	0.1509	0.1979

3.3. Validation results

In the initial modeling with two turbulence models, the model was implemented and compared with the laboratory results so that the best and most similar results compared to the laboratory work are the basis for subsequent modeling in this field. After specifying the meshing conditions of the models, five experiments were examined to determine the best turbulence model and to evaluate the performance of the best turbulence transfer model. three parameters RMSE, MAE, and R^2 were used for the flow head parameter between the numerical and laboratory models. Thus, based on the obtained results it can be concluded that the numerical model is capable of simulating the three-dimensional flow on the weirs of the PKWs with reasonable accuracy and the results of the analysis of this flow by the numerical model can be relied upon. Also, Figure 6 shows the time variation diagram of the flow passing through the outlet boundary of the model. one of the signs of the stability of the model is the equality of discharge at the inlet boundary and the outlet boundary.

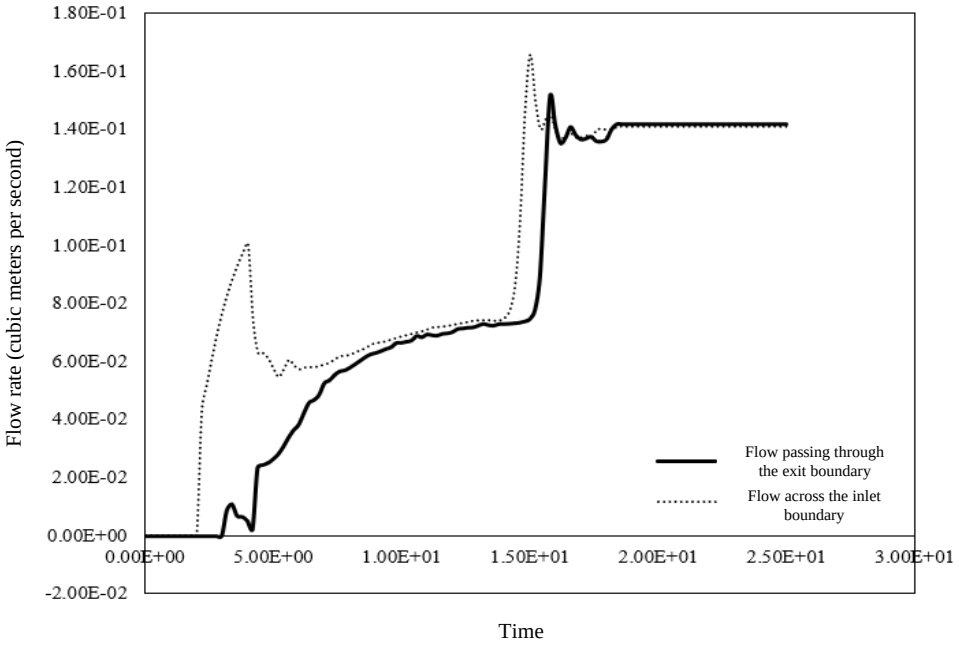

Figure 5. Time variation graph of the flow passing through the entrance and exit boundary of PKW for scenario Q-H_3.

As can be seen in Figure 5 the model has reached stability in the 18th second. In the following, the results of the flow simulation will be presented and analyzed.

3.4. New simulations on the PKW

In order to increase the efficiency of weirs, there are various solutions, three of the most important of these solutions are (Anderson and Tullis, 2012):

- Increasing the width of the overflow (W): It cannot be used in most cases due to the limitation of space.
- Reducing the height of the weir crest (P): this action has reduced the capacity of the dam reservoir, so it is not compatible with the goals of building larger reservoirs.
- Extending the length of the weir crest (L): in a certain width and fixed level of the support, they can be implemented by replacing linear weirs with non-linear ones, such as labyrinth and PKWs.

According to the cases mentioned above, it seems that to check the geometrical parameters affecting the hydraulic performance of weirs, it is necessary to keep the width of the weir constant in the models provided by each researcher. It may not be economical from an economic point of view, so it can be concluded that among the weirs models presented by each researcher (assuming that all the geometrical parameters are constant for all models) the weir that can achieve the highest discharge at the lowest flow head and in the shortest possible weir length is superior. It is obvious that to compare the effect of a geometric parameter in different models it is necessary to consider other parameters as constant for all models, for example, if the effect of the channel width parameter is to be determined for several different values (W=1, W=2 and W= 3) and it should be examined for several different models, to better understand the effect of changes in the mentioned parameter, it is better to consider other parameters such as the height of the weir, the length of the weir, etc. as constant for other models, otherwise, it is not possible to comment on the effects of changing that parameter. After studying many theses and articles, whose purpose was to

investigate the geometric parameters of the PKW, it was observed that most of the researchers did not consider the points mentioned above, and practically comparing the equality between the models have not created themselves that this can cause problems in the evolutionary process of achieving the best design method of PKWs. By placing the weir of the PKWs on the arced line, the keys necessarily change in trapezoid shape (ATPKW). Figure 6 shows the general geometry of the PKW with an arc plan. Also, Table 6 shows the parameters used in Figure 6.

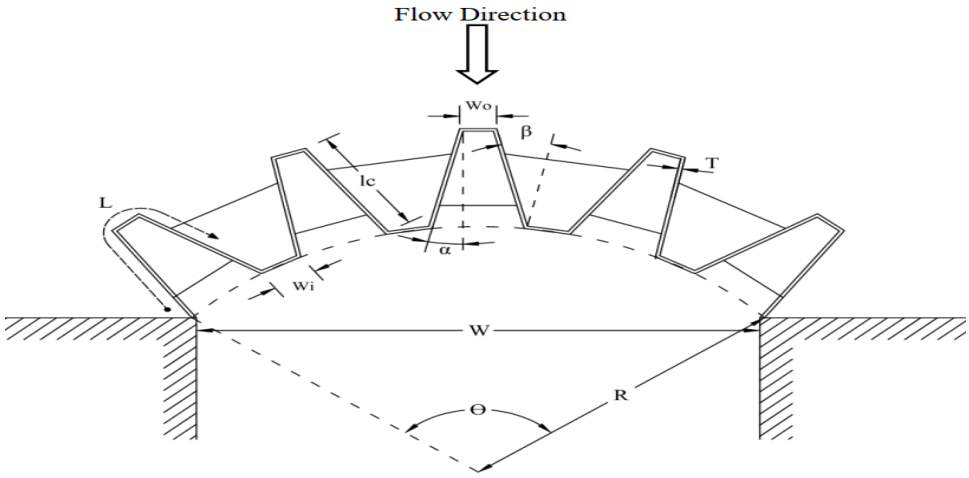

Figure 6. Geometrical parameters of arced trapezoidal piano key weir (ATPKW) in plan.

Table 6. Parameters used in weir geometry.

parameter	Description
θ	weir angle
R	radius of arc
α	Outlet key angle
β	Inlet key angle
W	weir width
w_i	Inlet key width
w_o	Outlet key width
B_i	The length of the inlet key console
B_o	The length of the outlet key console
l_c	The length of the lateral crest
L	The length of the weir crest
T	The thickness of the weir wall
N	Number of cycles

In this part of the research, the hydraulic behavior of this type of weir has been studied by changing the parameters of the number of cycles and the weir angle. Weirs are modeled for four central angles of 45, 90, 135 and 180 degrees and the number of cycles 2, 3 and 4. It should be noted that one of the strengths and distinctions of this research with other researches in this field is keeping all the effective parameters, including the overall length of the weir (L) constant in all models. Also, in all models, the weir width (W) and crest height (P) are fixed. Since we want to examine the effect of simultaneous changes in the number of cycles and the weir angle, the correct comparison is done when the effect of other effective parameters is removed. In the continuation of the research, the weir results of the ATPKWs have been compared with its linear models researched by Anderson. Table 6 presents different models and their geometric parameters. Figure 7 shows the three-dimensional view of weirs. It should be noted that the reservoir upstream of the weirs is considered large enough so that the borders of the field are not affected by the currents approaching the weir.

Table 7. Geometrical parameters ATPKWs.

Model	Parameters																	
	θ	N	P	L	W	lc	Wi	Wo	Wi/Wo	Si	So	α	β	Bi/lc	Bi	Bo	T	L/W
ATPK-45-2	45	2	0.1969	4.7454	0.932	1.01	0.20	0.20	1	55.56%	55.56%	11	14	0.1202	0.1214	0.1214	0.0127	5.092
ATPK-45-3		3				0.67	0.13	0.13				17	17	0.18119				
ATPK-45-4		4				0.51	0.09	0.09				8	3	0.23804				
ATPK-90-2	90	2				0.96	0.21	0.21				20	25	0.12646				
ATPK-90-3		3				0.64	0.14	0.14				3	3	0.18969				
ATPK-90-4		4				0.48	0.10	0.10				9	14	0.25292				
ATPK-135-2	135	2				0.938	0.25	0.25				31	37	0.12942				
ATPK-135-3		3				0.639	0.16	0.16				3	3	0.18998				
ATPK-135-4		4				0.482	0.12	0.12				14	20	0.25187				
ATPK-180-2	180	2				0.88	0.30	0.30				40	50	0.13795				
ATPK-180-3		3				0.586	0.20	0.20				5	4	0.20717				
ATPK-180-4		4				0.443	0.15	0.15				18	27	0.27404				

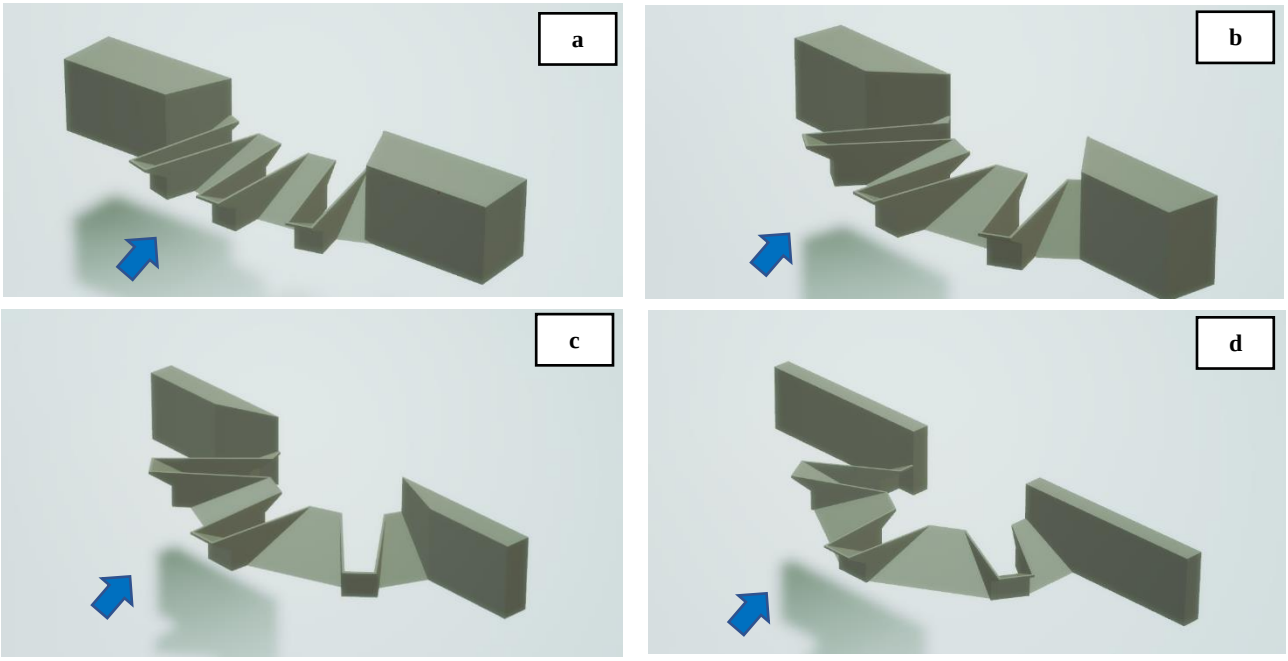

Figure 7. Three-dimensional view ATPKWs with three cycles in plan **a**) 45 degrees **b**) 90 degrees **c**)135 degrees and **d**) 180 degrees.

4. Results and discussion

Figure 8 shows the changes of the discharge coefficient against the ratio of the head to the height (H/P) of the ATPKWs in the plan for different angles of the weirs set for the number of cycles two and Figures 9 and 10 are the same for the number of cycles three and four. In all weirs, the crest length is equal (L=Constant). As can be seen in Figure 8 the weir with an angle of 135 degrees and two cycles has a better performance than other weirs so the value of the discharge coefficient for this weir is 0.87. On the other hand, with the increase of the weir angle in a constant cycle is the trend of changes in the discharge coefficient up to an angle of 135 degrees, and from then on it has a downward trend. It can also be seen from Figure 8 that the highest discharge coefficient occurs in the ratio of head to weir height (H/P) equal to 0.2. According to Figure 11, the creation of curvature in the weir plan compared to the linear PKWs (Anderson models) has improved the hydraulic performance of the weir in such a way that the effect of the curvature is high for low heads and in high heads there is a significant difference between the coefficient There are no arced and linear weirs. The greatest effect of the curvature of the crest is for the head-to-height ratio (H/P) of 0.2 so that the discharge coefficient has increased from 0.42 to 0.87.

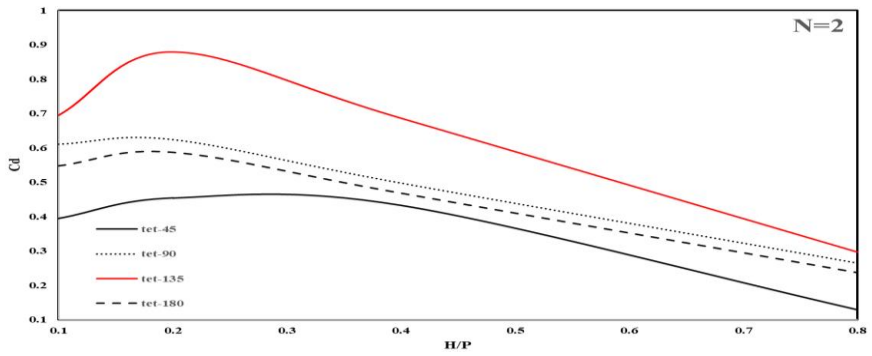

Figure 8. Comparison of discharge coefficient of weirs with 2 cycles and the same weir crest length.

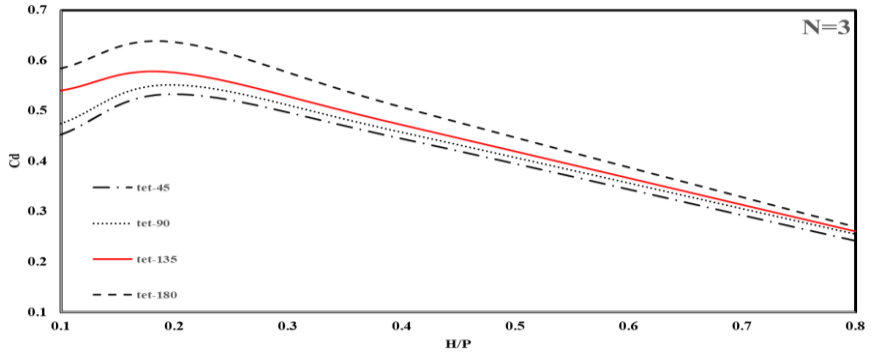

Figure 9. Comparison of discharge coefficient of weirs with 3 cycles and the same weir crest length.

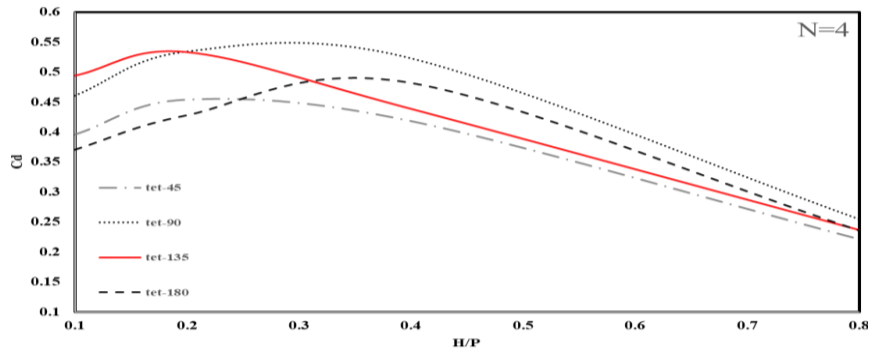

Figure 10. Comparison of the water passage coefficient of weirs with 4 cycles and the same weir crest length.

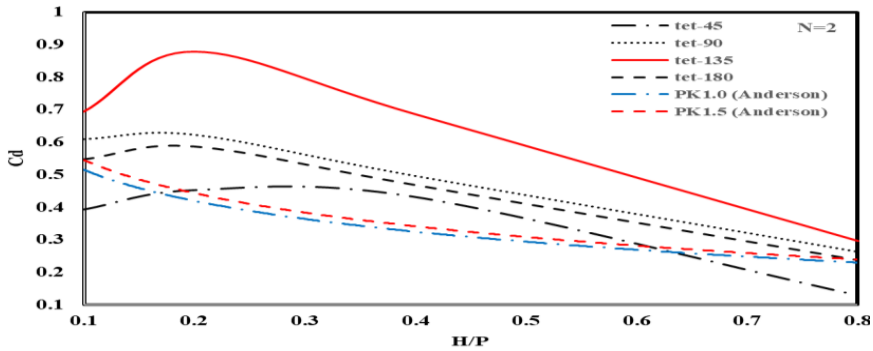

Figure 11. Comparison of discharge coefficient of the weirs of the present research and the samples of Anderson's linear PKWs.

Figures 12 to 14 show the three-dimensional pattern of flow from different angles on the ATPK135-3 weir for different heads. In the lower heads, the major part of the flow is discharged from the outlet keys, and also in the flow approaching the weir, the water level is horizontal and no drop is observed. With the increase of the water head on the weir, the outlet keys are submerged and as shown in Figure 13 with the increase in the volume of flow passing through the side keys, the flow speed also increases and the falling flow collides at higher levels. The result of the collision of the falling flow on the sides is the rise of the water level in the upper layers inside the outlet keys and the formation of strong local submergence in the mentioned areas. According to Figure 14, the formation of local submergence causes a reduction in the width of the flow passing through the outlet key and the flow passing through the outlet key only passes through the sides of the intersection of the falling flows inside the outlet key. It should be noted that the phenomenon of local submergence somehow reduces the effective length of the weir and causes a decrease in the hydraulic performance of the spillway as well as a decrease in the discharge coefficient. Figure 14 shows well how the local submergence of the outlet key increases in proportion to the increase in flow head. The parameter indicating the progress of local submergence in the mentioned figure is called fluid fraction, which is denoted by F in short. The volume of fluid (VOF) technique is based on the idea of recording in each grid cell a fraction of the cell volume occupied by liquid. Since volume is a fraction, F must have a value between 0 and 1. In regions inside the fluid, the value of F will be equal to 1 while outside the fluid in regions of gas (eg air), the value of F is zero. As mentioned before, local submergence occurs when the flow passing through the outlet key collides with the flow passing through the side crest of the keys.

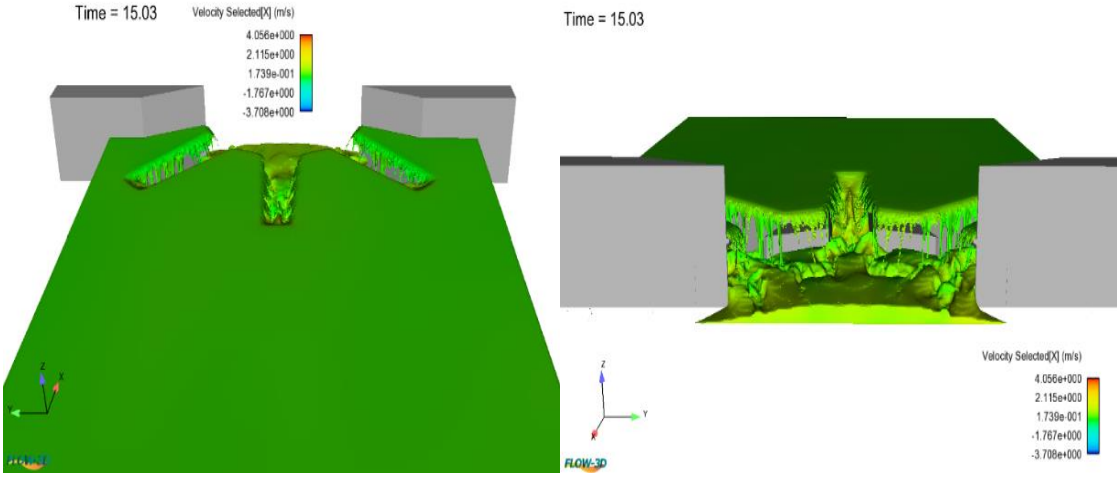

Figure 12. 3D pattern of free flow and view from the ATPK 135-3 weir at H/P = 0.1.

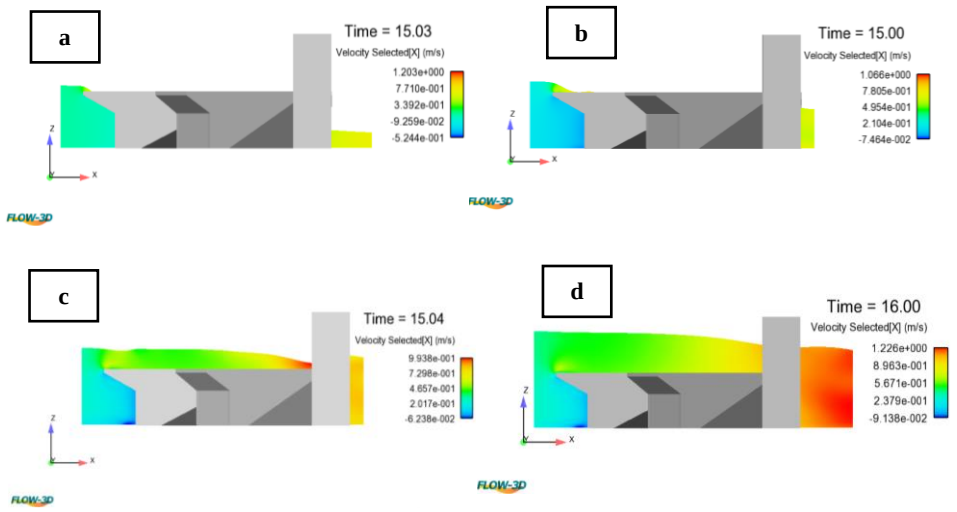

Figure 13. Two-dimensional flow pattern in the X-Z plane for different heads **a**) H/P=0.1 **b**) H/P=0.2 **c**) H/P=0.4 **d**) H/P=0.8.

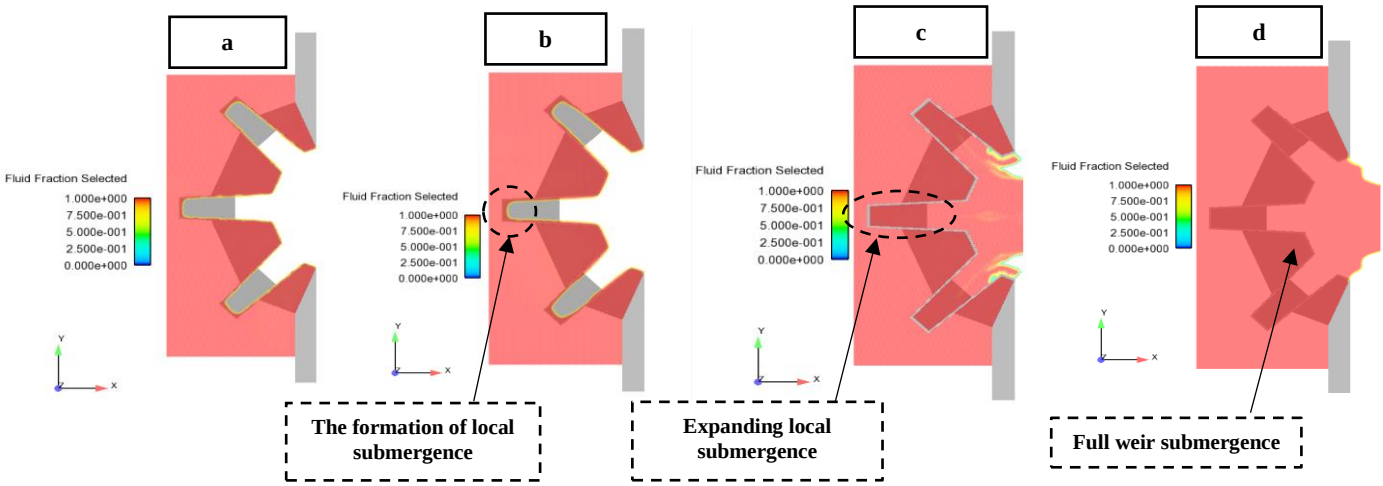

Figure 14. How to increase the local submergence of the outlet key in ATPK-135-3 weir according to the increase of the flow head **a**) H/P=0.1 **b**) H/P=0.2 **c**) H/P=0.4 **d**) H/ P = 0.8.

Figure 15 shows the streamlines in the lower and middle levels of ATPK45-2 and ATPK135-2 weirs. As can be seen, in the mentioned weirs after reaching the inlet key the lower flows are uniformly distributed on the side crests and the inlet key, of course, a better flow distribution can be seen for the ATPK135-2 weir. Regarding the flows approaching the side keys for the mentioned weirs, as can be seen, the flow passes through the entrance key with a proper distribution but some of the streamlines approaching the central key are drawn towards the side keys and change direction to the upper layers and then passes through the side crest of the weir side keys. In these areas, the flow velocity decreases and the flow recirculates. One of the reasons for this is the angular sides of the weir foundations and the distance created between the sloping surface and the place of flow transfer from the tank to the inlet key. The creation of the recirculation area in the inlet key reduces the effective width of the flow in the inlet key. Figure 16 shows the streamlines of the lower layer for ATPKWs with an arc cycle angle of 135 degrees and in different

cycles. As can be seen, with the increase in the number of cycles (at a fixed weir angle and length) the streamlines in the inlet key become more constricted and the distribution of the streamlines with more compression is formed on the side crests of the inlet keys which causes the flow to collide. Falling from the side crests causes the flow to decrease as well as increase the upstream head. Figure 17 shows the approaching middle layer streamlines for ATPKWs with an arc cycle angle of 135 degrees and in different cycles. The upper layers of the flow tend to pass through the outlet key but as seen in Figure 17 with the increase of the cycle and especially in cycles 3 and 4 the streamlines use the capacity of the outlet key while in cycle 2 due to the drainage area most inlet key streamlines make good use of the capacity of the inlet key side crests and keep the outlet key capacity for higher layer flow. Figure 18 shows the flow velocity distribution (in the upper layer of the flow and under the crest) in the inlet key for the weir with an angle of 135 degrees and H/P = 0.4. As can be seen, in the second cycle the velocity distribution is more uniform in such a way that the streamlines pass almost vertically through the side crest, and all the capacity of the side crest is well used. Also, the main reason for the more uniform speed distribution in the second cycle is the increase in the intake level of the inlet key (or increase in the area of the inlet key) is in the second cycle and this phenomenon reduces the inertia of the flow along the inlet key and creates better conditions for the discharge of the flow in the side crests.

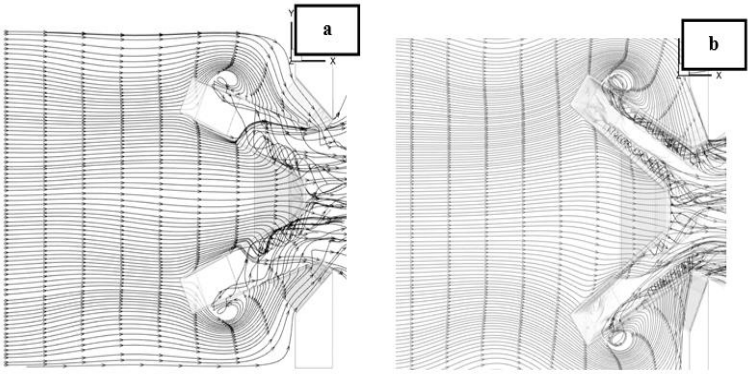

Figure 15. stream lines of the lower layer of the weir **a**) ATPK45-2 **b**) ATPK135-2.

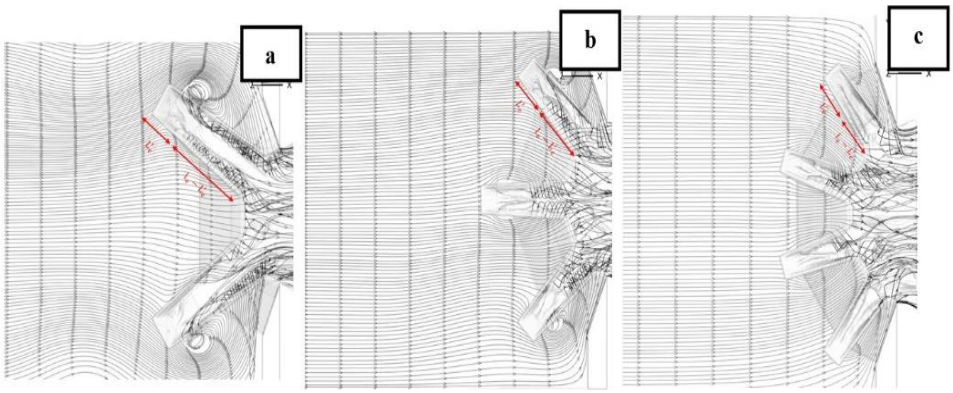

Figure 16. stream lines of the lower layer in the overflows of the ATPKW with an angle of 135 degrees and the number of cycles **a**) two **b**) three **c**) four.

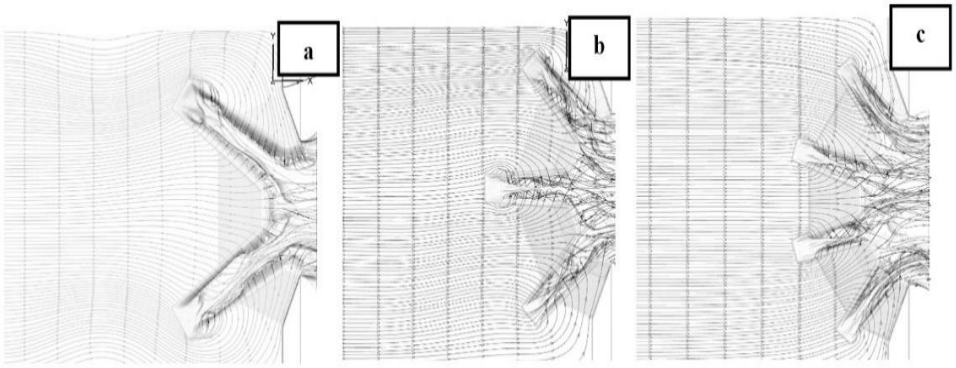

Figure 17. The stream lines of the middle layer in the overflows of the ATPKW with an angle of 135 degrees and the number of cycles **a**) two **b**) three **c**) four.

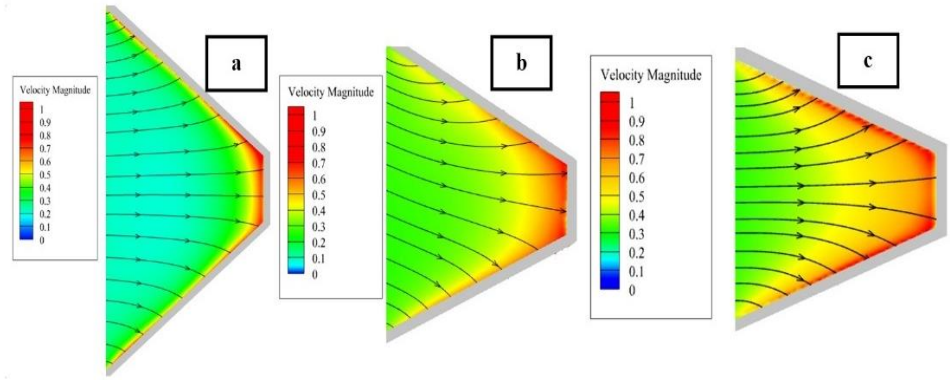

Figure 18. Distribution of the flow velocity of the upper layer (under the crown) in the inlet key for H/P = 0.4 for the overflow with an angle of 135 degrees a) Two cycles b) three cycles c) four cycles.

Figure 19 shows the changes in the discharge coefficient of the ATPKWs researched by B.Noroozi (Safarzadeh and Noroozi, 2017), Thomas Anderson (Anderson and Tullis, 2012), the current research and the PK1.0 weir (which is linear) against the head to the height of the weir and the Head-Discharge curve. As can be seen, ATPK135-2 and APK150-5 have a higher water discharge coefficient than the linear PKWs tested by Anderson and this is in the case that the total length of ATPK135-2 is equal to 4.7 meters, APK150 equal to 5.9 meters (Safarzadeh and Noroozi, 2017), PKFH equal to 4.7 meters (Anderson and Tullis, 2012) and PK1.0 equals 4.7 meters. It should be noted that other geometrical parameters such as crest height (P), wall thickness (T), and the width of the weir construction (W), etc. are the same for all the mentioned weirs except the APK150-5 weir provided by B.Noroozi. For the APK150-5, the width of the weir construction (W) is equal to 1.49 meters and for the other mentioned weirs it is equal to 0.93 meters. What can be obtained from the information about the compared weirs is that the APK150-5 spillway is geometrically superior to other spillways and it is expected to have a better hydraulic performance which of course is not the case. The ATPK135-2 with the minimum total length has been able to obtain a higher water discharge coefficient than the APK150-5, which indicates the importance of local submergence effects formed in the outlet key for PKWs. As can be seen in the Head-Discharge curve for the APK10 weir of B.Noroozi (which includes 10 cycles and the total length of the weir is equal to 11.87

meters and actually has dimensional superiority compared to other weirs in the mentioned diagram) the flow rate passing over the weir increases. It was found and also for higher heads, this trend is completely upward and the volumetric intensity of the flow passing over the weir increases with a steeper slope. For the ATPK135-2 the flow rate passing through the weir is upward but at higher heads the volumetric intensity of the flow passing through the weir continues with a slower slope, but for the PK1.0 Anderson linear weir with the increase of the flow head, the volumetric intensity of the flow passing through the weir is lower than other but it continues at a constant rate. From the Head-Discharge diagram of the mentioned weirs it can be seen that the increase in the gradient of the volumetric intensity of the flow passing over the weir indicates the increase of the local submergence area in the outlet keys of the weir and it causes a decrease in the hydraulic efficiency of the weir and practically the greater gradient of the volumetric intensity of the flow passing over the weir, the weir loses its efficiency sooner. We know that one of the goals of designing overflows should be to achieve the best result with the lowest cost and it was found that the phenomenon of local submergence can make this principle difficult in designs and impose additional costs on the designer and manufacturer.

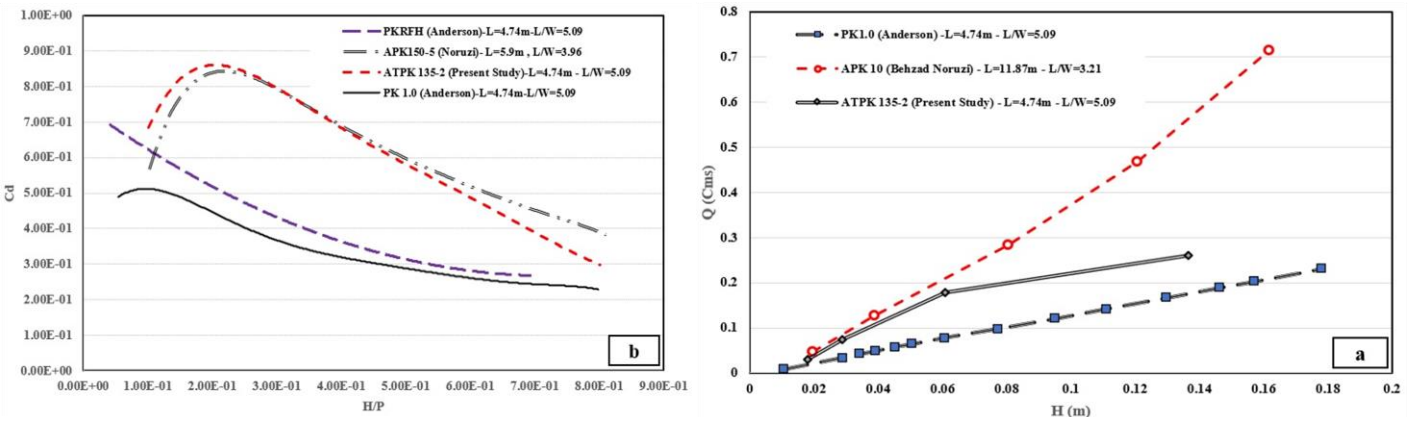

Figure 19. (**a**) Head-Discharge curve of the weirs discussion topic (**b**) Changes in the discharge coefficient of ATPKWs researched by B.Noroozi (Safarzadeh and Noroozi, 2017), R.M.Anderson (Anderson and Tullis, 2012), present research and PK1.0 Weir (which is linear) against the head to the height of the weirs.

As can be seen in Figure 20, by increasing the angle of the weir or in other words by decreasing the radius of curvature with the overall length of the weir crest being constant, the amount of flow passing through the ATPKWs has increased and on the other hand with the increase in the number of cycles with the overall length of the weir crest being constant and the value of the flow passage coefficient has a downward trend which is the reason for the reduction of the area of the inlet water catchment. The above-mentioned points are directly related to the flow pattern passing through the weirs of the subject of the present research and regarding the investigation of their hydraulic performance. the general pattern as well as the stream lines are discussed on them.

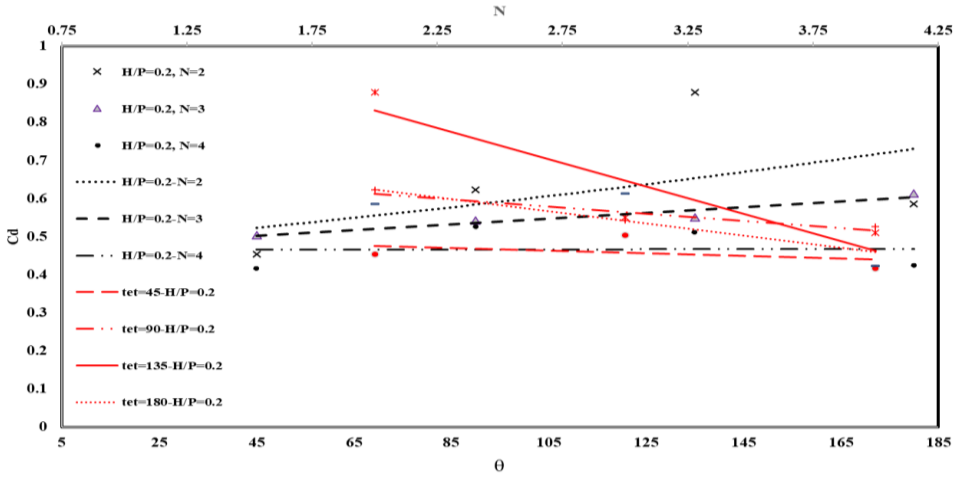

Figure 20. Comparison of the discharge coefficient of ATPKWs against the effect of increasing the cycle and weir angle for the same crest length of all weirs.

5. Multiple regression analysis

In the previous sections, the influence of parameters such as the number of cycles and the weir angle on the performance of the ATPKWs was studied and it was found that the discharge coefficient (C_d) is not dependent on only one variable. In the estimation of C_d all influential parameters should be involved as much as possible and practically the effect of changes of all parameters on C_d should be considered. Therefore, the parameters that change by changing the number of cycles and the value of the weir angle for each observation are considered and after making them dimensionless and they are used as independent variables to fit the relationship. The purpose of this part of the study is to predict and express the changes of the C_d variable based on the information of other variables. In order to predict the changes of C_d variable multiple regression methods were also used which will be discussed in the following (Johnson and Bhattacharyya, 2019).

5.1. General relationship of multiple regression

In general, linear regression provides the estimation and inference results of $\beta = [\beta_1, \beta_2, \dots, \beta_p]^T$ parameters in the following pattern (Bornstein, 1986):

$$Y_n = \beta_0 + \beta_1 x_{n1} + \beta_2 x_{n2} + ... + \beta_n x_{np} \quad (6)$$

In the above model, β_0 is equivalent to the constant of the model, β_P is equivalent to the coefficient of the regression line, and X_{np} is equivalent to the independent variable. A non-linear regression model can be written as the following relation:

$$Y_n = \beta_0 + f(x_n, \beta) = \beta_0 + \beta_1 x_1 + \beta_2 x_2^{\,2} + ... + \beta_n x_n^{\,n} \quad (7)$$

In the above model, f is the expectation function and X_n is a vector containing regression or independent variables for the n state.

5.2. Conditions for using the multiple regression analysis method

In order to use the multiple regression analysis method, there must be the following six conditions (Johnson and Bhattacharyya, 2019) because if one of the conditions is violated the established regression relationship will suffer. In this research, two independent parameter groups have been used in order to derive mathematical relationships in order to estimate the value of discharge coefficient (C_d). The first group includes parameters H/P (ratio of flow head to weir height), L/Wi (ratio of weir length to the width of the entrance key) and L/lc (ratio of weir

length to the length of the side crest) and the second group H/P parameters, θ (weir angle) and N (number of cycles). It should be noted that C_d is also considered as a dependent variable. In order to create a proper regression between the stated independent parameters and the dependent parameter there must be six conditions as follows:

5.2.1. Checking the normality of dependent variables

In order to check the normality of the observations of the dependent variable which in the present research is the discharge coefficient (C_d) it is necessary to check the skewness and kurtosis test to check the z-statistic of skewness and the z-statistic of kurtosis. to be Relations (8) and (9) are also related to the calculation of z-kurtosis and z-skewness. It should be noted that the value of Z should be between -1.96 and 1.96. In the following table 8 includes values of skewness and kurtosis as well as values of standard error (S.E) of skewness and kurtosis (Gravetter and Wallnau, 2014; Johnson and Bhattacharyya, 2019).

$$Z_{skewness} = \frac{Skewness}{(S.E)Skewness} \quad (8)$$

$$Z_{Kurtosis} = \frac{Kurtosis}{(S.E)Kurtosis} \quad (9)$$

Table 8. Values and standard error of skewness and kurtosis of the dependent parameter.

parameter	rating
Skewness value	0.0121
Standard error of the skewness	0.3431
kurtosis value	0.1669
standard error of kurtosis	0.6744

According to the relations 8 and 9 and the values in table 8 the value of the skewness Z statistic is equal to -0.34 and the value of the kurtosis Z statistic is equal to -0.23 and the values in mentioned interval is also located. The diagram in figure 21 shows the histogram of the normality of observations of the dependent variable (C_d).

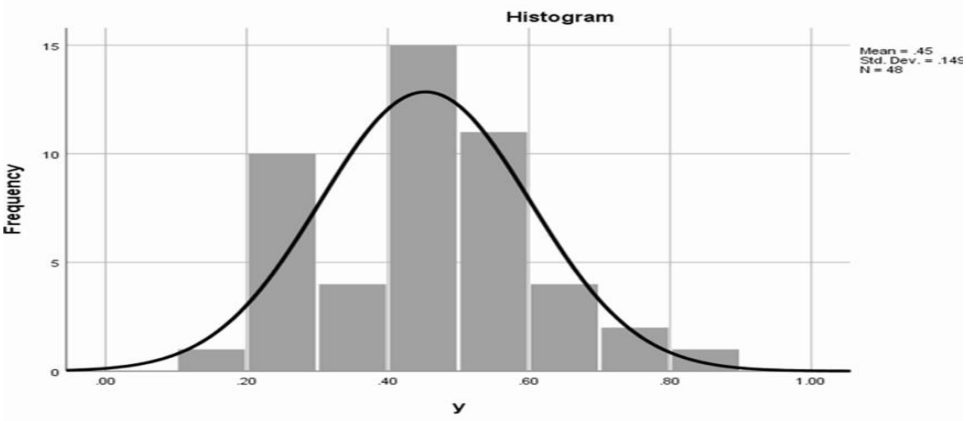

Figure 21. Histogram of normality of dependent variable observations.

5.2.2. Examining the normal distribution with constant variance for the amount of residuals

In examining the normal distribution of the data, we have two hypothetical tests H_0 and H_A and the hypothesis H_0 shows that the distribution of observations is normal and the hypothesis H_A shows the existence of a non-normal distribution in the observations (Johnson and Bhattacharyya, 2019). It should be noted that the permissible error of the test is also equal to 0.05. After specifying the variable results of Kolmogorov-Smirnov and Shapiro-Wilk methods can be used. According to the value of the significant level, the assumption of H_0 and H_A can be checked with an error value of 0.05. In other words, if the significance level value of the variable is greater than 0.05, as a result, the assumption H_0 of the test is valid and there are no sufficient conditions to violate the test. In this section, it should be noted that if one of the mentioned methods considers the assumption H_0 to be valid the normality of the variable has been proven. Table 9 includes the values of the Kolmogorov-Smirnov and Shapiro-Wilk methods to check the normality of data distribution. The graph of figures 22 and 23 also shows the test of normal distribution of data. As can be seen, condition H_0 is satisfied.

Table 9. The values of the Kolmogorov-Smirnov and Shapiro-Wilk methods to check the normality of the data distribution of the first and second groups.

	Shapiro-Wilk method		**Kolmogorov-Smirnov method**	
	The significance level	Number of observations	The significance level	Number of observations
Non-standard error of the first group of data (H/P-L/Wi-L/lc)	0.164	48	0.070	48
Non-standard error of the second group of data (H/P- θ-N)	0.163	48	0.130	48

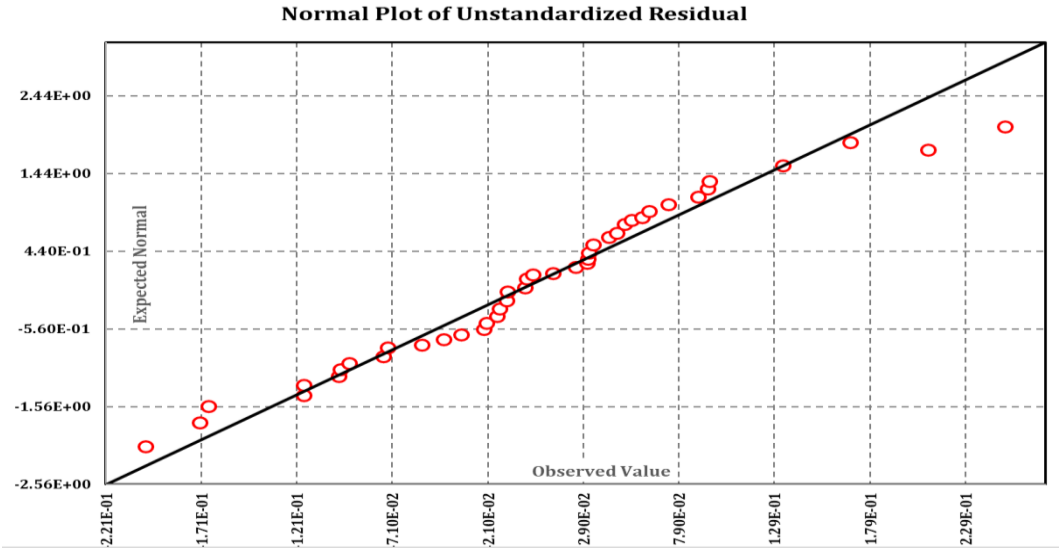

Figure 22. Normal distribution diagram of observed values for the first group of data.

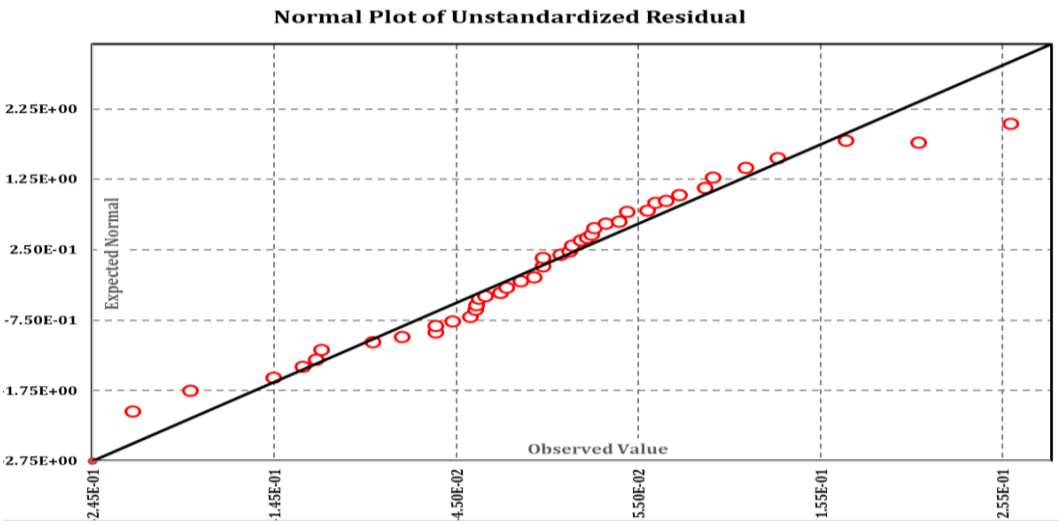

Figure 23. Normal distribution diagram of observed values for the second group of data.

5.2.3. Checking the autocorrelation between the residuals

Auto correlation or serial correlation is a mathematical concept that is used to find repeating patterns such as the presence of a signal or wave that is hidden under noise (Gravetter and Wallnau, 2014; Johnson and Bhattacharyya, 2019). Durbin-Watson statistic is used to check the existence of autocorrelation. The value of the numerical statistic is between 0 and 4. Values close to zero indicate positive correlation and values close to 4 indicate negative correlation (Johnson and Bhattacharyya, 2019). Placing this statistic in the range of 1.5 to 2.5 indicates the absence of correlation or the presence of negligible correlation. As can be seen in table 10 there is no automatic correlation between the considered independent parameters.

Table 10. Autocorrelation value between independent parameters.

Models	Durbin-Watson values
Independent variables of the first group (H/P-L/Wi-L/lc)	1.63
Independent variables of the second group (H/P- θ-N)	1.52

5.2.4. Collinearity check between independent variables

The existence of strong correlation between independent variables actually indicates the existence of a linear relationship between them (Johnson and Bhattacharyya, 2019). In this case, the coefficients obtained from the mathematical model are not real and cause problems in the predictions. If we succeed in discovering the relationship between independent variables, we should avoid using correlated variables as much as possible and use fewer variables in the model. To check this type of correlation, use the variance inflation factor (VIF) or the tolerance coefficient. The variance inflation factor determines how much the variance of the estimated regression coefficient is greater than when the independent variables are truly independent of each other. The variance inflation factor is always greater than or equal to one. It should be noted that values close to

one indicate independence and non-collinearity and values greater than 10 indicate strong collinearity between variables. The tolerance coefficient is the value of the variance of the independent variable that is not predicted by other independent variables. Values less than 0.1 for the tolerance coefficient indicate a strong correlation between independent variables, and in this case, the choice of independent variables should be reconsidered. The following table 11 shows the values of the variance inflation factor and the tolerance coefficient for the considered independent variables.

Table 11. Values of the variance inflation factor and the tolerance factor for the considered independent variables.

Independent parameter		Variance inflation factor (VIF)	Tolerance factor
First group	H/P	1	1
	L/Wi	2.212	0.452
	L/lc	2.212	0.452
Second group	H/P	1	1
	θ	1	1
	N	1	1

5.2.5. Checking the absence of outlying observations in the data set

An outlier observation is an observation that does not follow the conventional pattern of observations, and it is better to remove these observations from the data (Johnson and Bhattacharyya, 2019). From a technical point of view, an outlier is an observation that is more than 3 standard deviations away from the mean. Statistically, the value of 3 standard deviations means the value of 95% of observations is covered. In the present research, no outliers were observed for the data.

5.3. Correlation

The correlation coefficient shows the intensity of the relationship and its direction between two variables. The correlation coefficient is as follows:

$$\rho_{xy} = \frac{\sum_{i=1}^{n}(x_i - \overline{x})(y_i - \overline{y})}{\sqrt{\sum_{i=1}^{n}(x_i - \overline{x})^2 \sum_{i=1}^{n}(y_i - \overline{y})^2}}, \rho_{xy} = \rho_{yx} \quad (10)$$

It should be noted that values of correlation coefficient close to +1 indicate strong positive correlation and values close to -1 indicate strong negative correlation. The mentioned statistic in multiple regression is shown as coefficient of determination R^2. The coefficient of determination states how many percent of changes in the dependent variable are determined by the independent variables. In other words, the coefficient of determination shows how much of the dependent variable's changes are influenced by the independent variables and how much of its changes are related to other factors. It should be noted that the coefficient of determination R^2 will naturally increase with the increase of the number of independent variables which is considered a statistical problem and to avoid this problem the adjusted coefficient of determination $R^2_{adjusted}$ is used. It should be noted that the smaller the difference between $R^2_{adjusted}$ and R^2 indicates the right choice of independent variables.

5.4. Regression model significance test

The statistical hypothesis test device is written as follows in order to check the significance

of the regression model (Bornstein, 1986; Gravetter and Wallnau, 2014; Johnson and Bhattacharyya, 2019):

$$\begin{cases} H_0 : \beta_0 = \beta_1 = \beta_2 = ... = \beta_K = 0 \\ H_A = \text{At least one tie is not established} \end{cases} \quad (11)$$

In the significance analysis of the regression model, the total changes can be divided into two parts: changes caused by independent variables and changes related to errors and other random factors. As a result, the more the changes by the independent variables are more than the error changes, the more suitable the regression line is, otherwise the regression line is not suitable. If the value of the significant level is zero (or less than 0.05), it means that the null hypothesis of the above statistical test is violated, and as a result, at least one of the coefficients of β is not zero, and in fact, the coefficients of β are significant. Table 12 shows the values of the significance level for the coefficients of the linear regression relationship. As can be seen, all the coefficients are significant and non-zero.

Table 12. Significant level values for regression coefficients.

Independent parameter		Coefficient values	Standard error	The significance level
First group	**Constant**	0.541	0.119	0
	H/P	-0.419	0.048	0
	L/Wi	2.779	0.063	0.023
	L/lc	-0.004	0.811	0.048
Second group	**Constant**	0.754	0.119	0
	H/P	-0.419	0.049	0
	θ	-	0.007	0.74
	N	-0.048	0.016	0.005

5.5. Extracted regression relationships

According to the contents and points stated in the previous sections three regression relationships using independent parameters H/P, L/Wi and L/lc to calculate the value of the discharge coefficient (C_d) for ATPKWs. The condition of using the provided reports is that the width of the inlet key is equal to the outlet key (Wi=Wo) and the weir angle value is more than 45 degrees. In order to check the validity of the presented relationships, R^2, RMSE and MAE error functions have been used. Regarding the correlation coefficient R^2, RMSE and MAE, complete explanations have been provided in the previous parts and chapters. As can be seen in table 13 relation 11 is capable of more accurately predicting the discharge coefficient (C_d) for ATPKWs.

Table 13. The relationships presented to calculate the discharge coefficient (Cd) for ATPKWs.

	Calculation relations of discharge coefficient	R^2	RMSE	MAE	Relationship number
1	$C_d = 0.541 + 0.419(\frac{H}{P}) + 2.779(\frac{L}{W_i}) - 0.004(\frac{L}{l_c})$	0.68	0.127	0.104	(8)
2	$C_d = 0.336 - 0.592(\frac{H}{P})^{3.241} + 1.069(\frac{L}{W_i})^{0.466} - 0.004(\frac{L}{l_c})$	0.76	0.083	0.071	(9)
3	$C_d = -4.685 - 0.732(\frac{H}{P}) + 133.377(\frac{L}{W_i}) + 0.755(\frac{L}{l_c})$ $-795.842(\frac{L}{W_i})^2 + 0.041(\frac{H}{P})(\frac{L}{W_i}) - 9.126(\frac{L}{W_i})(\frac{L}{l_c})$ $-0.028(\frac{L}{l_c})^2$	0.87	0.071	0.056	(10)
4	$C_d = -0.301 - 0.588(\sqrt{\frac{H}{P}})^{6.330} + .008(Sin(\frac{\theta}{2})) + N^{-0.169}$	0.89	0.064	0.049	(11)

The diagram in figure 24 shows the trend of changes in the predicted and actual values of C_d per the number of observations related to the relation 10 and also the diagram in figure 25 of the error between the predicted values and the actual C_d for each observation related to relation 10 shows. By examining the above graphs, it is concluded that the average error occurred between the predicted and observed values is 12%. In the following, the graphs in figure 26 and 27 respectively show the scatter border of the observed values for C_d against the predicted values of relations 8 and 9. As can be seen in figures 26 and 27 the maximum dispersion limit obtained from relations 8 and 9 is equal to 23 and 18% respectively. The diagram in figure 28 is the scatter border for the observed values of C_d against the predicted values of the relation 11. As can be seen in figure 28, the maximum dispersion limit obtained from relation 11 is equal to 11%.

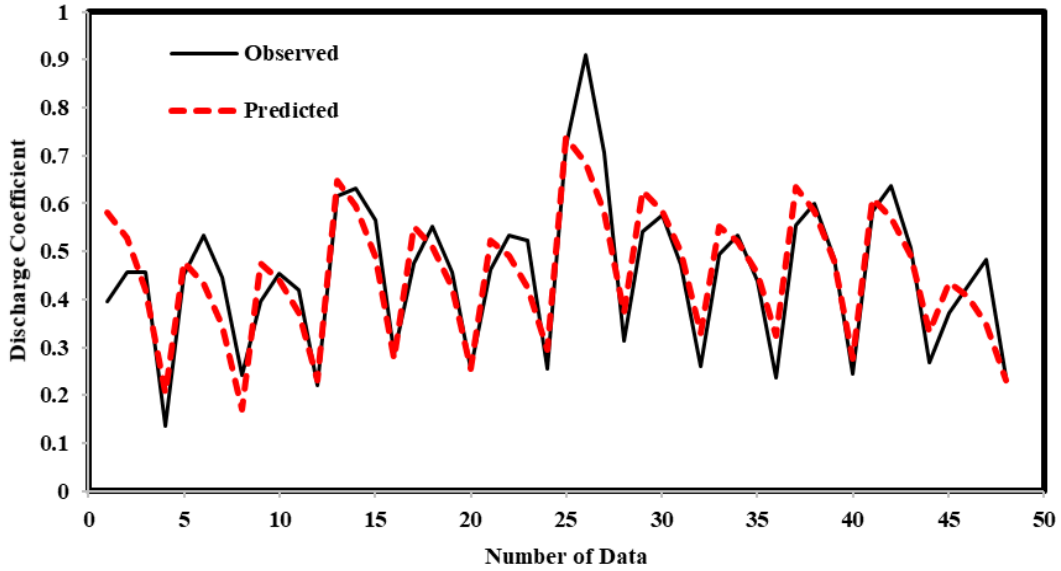

Figure 24. Changes trend of predicted and observed values of C_d coefficient per number of observations related to relation 10.

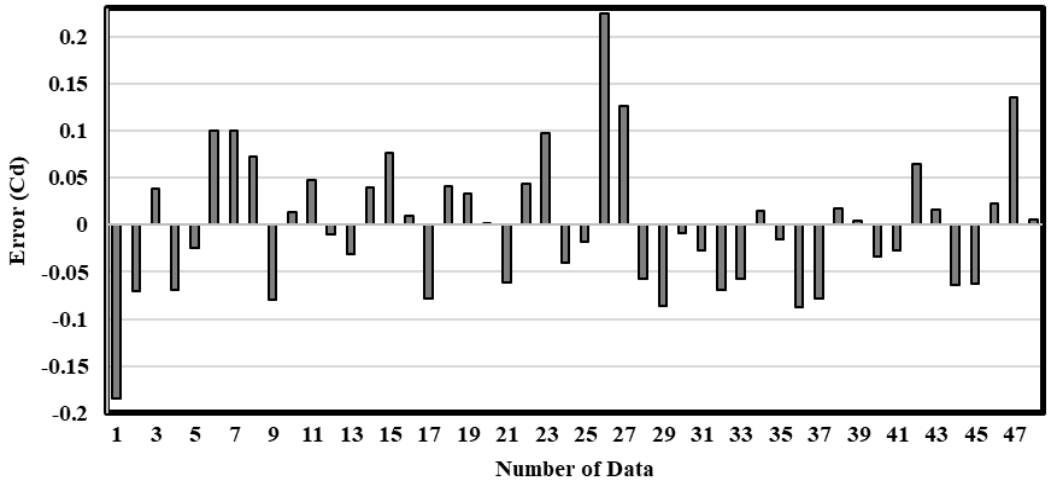

Figure 25. Error between predicted and observed values of C_d coefficient for each observation related to relation 10.

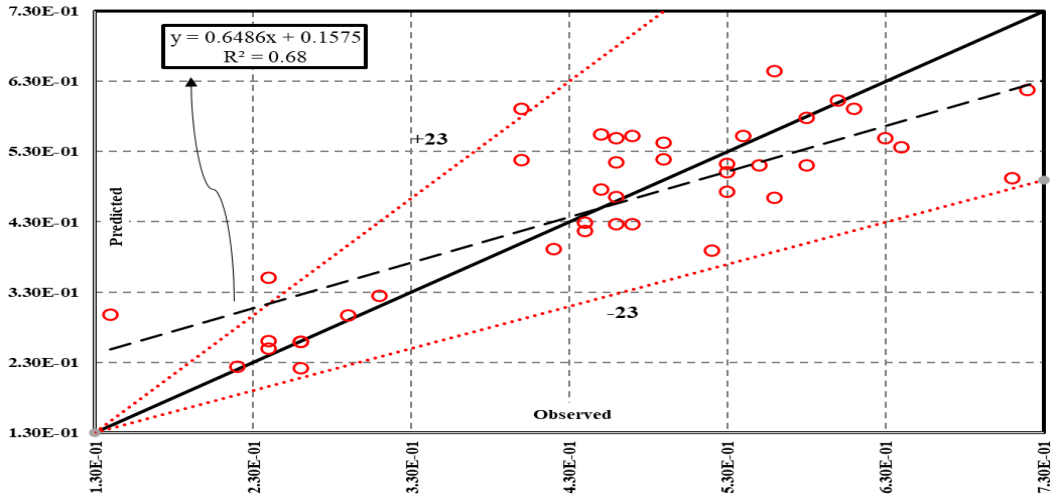

Figure 26. Comparison of observed and calculated values of C_d related to relation 8.

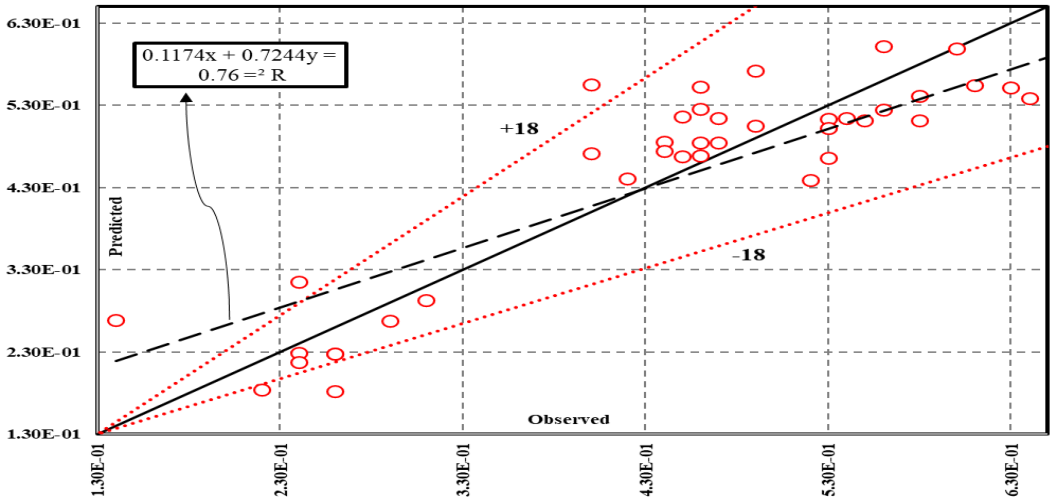

Figure 27. Comparison of observed and calculated values of C_d related to relation **9.**

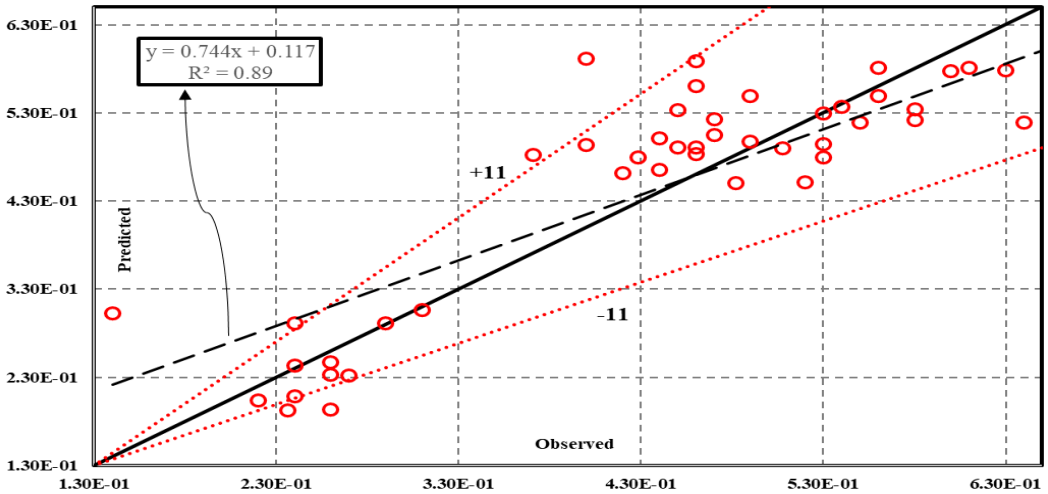

Figure 28. Comparison of observed and calculated values of C_d coefficient related to relation 11.

6. Conclusion

The purpose of the present research is to achieve the best geometry of the non-linear piano key weir with regard to spending the lowest cost (at least the total length of the weir). For this purpose, weirs in different angles and cycles and at the same time with the total length of the weir and the width of the building were modeled and simulated (for all models) and the results obtained are as follows:

- Comparing the performance of linear and ATPKWs showed that, in general, the discharge coefficient of ATPKWs is higher PKWs, and at high heads due to the submergence of the whole set, there is little difference in the hydraulic performance of the mentioned weirs.
- Curvature of the weir set changes the shape of the keys from rectangular to trapezoidal and this causes uniform distribution of stream lines, reduction of compression of stream lines and proper distribution of flow speed along the side crest of the inlet keys.
- In general, increasing the weir angle of the ATPKWs in a fixed length for all models causes an increase in the discharge coefficient, but on the contrary, with an increase in the number of cycles in a fixed length for all models, due to the reduction of the area of the inlet key, the increase in the contraction of the stream lines and as a result of the intensification of the local submergence in the outlet key, the discharge coefficient will decrease significantly.
- Among all the weirs modeled in this research, the ATPK135-2 is known as the best model and has been able to increase the discharge coefficient by 47% compared to the linear mode of the PK1.0 weir.
- In examining the effects of simultaneous changes in the weir angle and the number of cycles, one should pay attention to the economic efficiency of the design because in the present research it was found that increasing the total length of the weir, the number of cycles and the weir angle cannot necessarily lead to the achievement of a high discharge coefficient because in the sections it was mentioned before that the APK150-5 weir (reviewed by B.Noroozi) had a geometric advantage (the total length of the weir and the width of the building is larger) compared to the ATPK135-2 weir (the best model of this research) but it had a weaker hydraulic performance.
- In order to predict C_d coefficient values, H/P, L/Wi and L/lc parameters were selected as the first group of independent

variables and H/P, θ and N parameters were selected as the second group of independent parameters and before creating a regression between the mentioned parameters and the C_d coefficient (as a dependent parameter), first by conducting statistical studies on the observations, full assurance of the correct selection of the mentioned parameters was obtained. As a result, it was found that relation 11 establishes the best fit between independent and dependent variables.

Data Availability

The data used to support the findings of this study is available from the corresponding author upon request.

Conflicts of Interest

The authors declare that they have no conflicts of interest regarding the publication of this pape**r.**

References

Anderson, R., Tullis, B., 2012. Piano Key Weir: Reservoir versus Channel Application. Journal of Irrigation and Drainage Engineering, 138: 773-776. DOI:10.1061/(ASCE)IR.1943-4774.0000464

Bornstein, M.H., 1986. Journal of Aesthetic Education, 20(2): 120-122. DOI:10.2307/3332707

Chahartaghi, M.K., Nazari, S., Shooshtari, M.M., 2019. Experimental and numerical simulation of arced trapezoidal piano key weirs. Flow Measurement and Instrumentation, 68: 101576.

Cicero, G., Delisle, J., 2013. Discharge characteristics of Piano Key weirs under submerged flow. Labyrinth and Piano Key Weirs II–PKW 2013: 101-109.

Crookston, B., Anderson, R., Tullis, B., 2018. Free-flow discharge estimation method for Piano Key weir geometries. Journal of Hydro-Environment Research, 19: 160-167.

Gravetter, F.J., Wallnau, L.B., 2014. Essentials of Statistics for the Behavioral Sciences. Wadsworth, Cengage Learning.

Guo, X. et al., 2019. Discharge capacity evaluation and hydraulic design of a piano key weir. Water Supply, 19(3): 871-878.

Johnson, R.A., Bhattacharyya, G.K., 2019. Statistics: principles and methods. John Wiley & Sons.

Kumar, M., Sihag, P., Tiwari, N., Ranjan, S., 2020. Experimental study and modelling discharge coefficient of trapezoidal and rectangular piano key weirs. Applied Water Science, 10(1): 43.

Mehboudi, A., Attari, J., Hosseini, S., 2016. Experimental study of discharge coefficient for trapezoidal piano key weirs. Flow Measurement and Instrumentation, 50: 65-72.

Ouamane, A., F.Lempérière, 2008. The Piano Key Weir is the solution to increase the capacity of the existing spillways.

Ribeiro, M., Pfister, M., Schleiss, A., 2013. Overview of Piano Key weir prototypes and scientific model investigations, pp. 273-281. DOI:10.1201/b15985-37

Roache, P.J., 1994. Perspective: A Method for Uniform Reporting of Grid Refinement Studies. Journal of Fluids Engineering, 116(3): 405-413. DOI:10.1115/1.2910291

Safarzadeh, A., Noroozi, B., 2017. 3D hydrodynamics of trapezoidal piano key spillways. International Journal of Civil Engineering, 15: 89-101.

Yousif, A., 2020. Experimental Investigation On Hydraulic Performance Of Non-Rectangular Piano Key Weir (PKW).